

Measuring and segmentation in CT data using deformable models

Václav Krajíček

Faculty of Mathematics and Physics
Charles University, Prague
Malostranské nám. 25, 11800 Praha 1,
Czech Republic
vajicek@volny.cz

Josef Pelikán

Faculty of Mathematics and Physics
Charles University, Prague
Malostranské nám. 25, 11800 Praha 1,
Czech Republic
Josef.Pelikan@mff.cuni.cz

Martin Horák

Department of Radiology,
Bulovka Hospital, Prague
Budínova 2, 180 81 Praha 8 - Libeň,
Czech Republic
martin.horak@volny.cz

Abstract

Accurate measuring of physical properties of human body has great importance for determining the best treatment. Our work aims at measuring volumes of organs such as kidney or liver in image data obtained from computed tomography (CT). We take advantage of long-time research in the area of deformable models. We have developed parametric model using closed B-Spline curves and have formulated energetic equation for their iterative evolution. Interior and exterior intensity distributions are taken into account, together with upcoming shape and position of regions in neighbouring slices of multi-slice CT data. This approach does not require gradient information, which is unreliable in medical images.

Keywords: Deformable Models, Active Snakes, CT, Medical Segmentation, Volume Measurement.

1 INTRODUCTION

Computed tomography is a common tool for medical diagnostics. It simply produces images of a human body interiors. They serve in the same way as X-Ray images have done for a century. They are as badly readable as X-Rays for untrained observer. On the contrary, CT images offer much more information. They are based on calibrated 3D data (position and density), organized into slices in axial plane of human body. Typical example of CT image can be seen in Figure 1. Thanks to these features we can use them not only for rough idea of human interior, but also for precise measurements of volume.

Physical measures of human body can say a lot about man's health. Remember, that temperature of healthy body is about 36,5 °C. Higher temperature means that body is fighting with an illness. The same goes for volumes of organs. Noticeable changes up or down of kidney-volumes indicate their proper function or dysfunction. These changes can be observed after a long period between CT scannings and also depend on correct and objective evaluation of CT images.

We are trying to develop methods for fast, accurate and automatic kidney segmentation which is precondition for measuring the volume. Nature of CT data and variety of human body make this task rather difficult.

Permission to make digital or hard copies of all or part of this work for personal or classroom use is granted without fee provided that copies are not made or distributed for profit or commercial advantage and that copies bear this notice and the full citation on the first page. To copy otherwise, or republish, to post on servers or to redistribute to lists, requires prior specific permission and/or a fee.
Copyright UNION Agency – Science Press, Plzen, Czech Republic

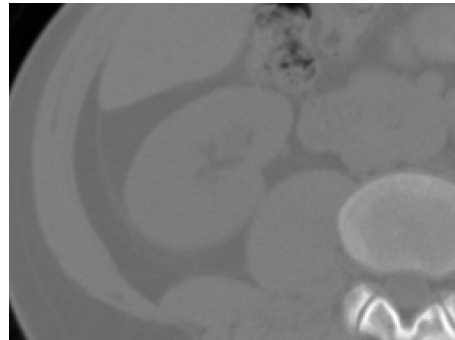


Figure 1: Slice of CT data from abdominal area.

2 RELATED WORK

Deformable models have been used and studied in computer vision for almost two decades. Their best known application is called 'active snakes' introduced in late 80's by Kass et al [KWT88]. They were based on evolving curves towards lowest total energy value defined mostly by image gradient and some regularization properties.

Unfortunately, medical images are very noisy and have unreliable gradient information. Chan and Vese [CV01] have introduced image energy term which depends on region statistics only.

$$E_{region1}(s) = \alpha \int_{int(s)} (f(x,y) - \mu_{ext}(s))^2 dx dy + \beta \int_{ext(s)} (f(x,y) - \mu_{ext}(s))^2 dx dy \quad (1)$$

Where s is closed curve, f is image and μ is mean intensity of exterior an interior area we want to separate. In this case μ can be known a priori or computed from initial position and updated during evolution.

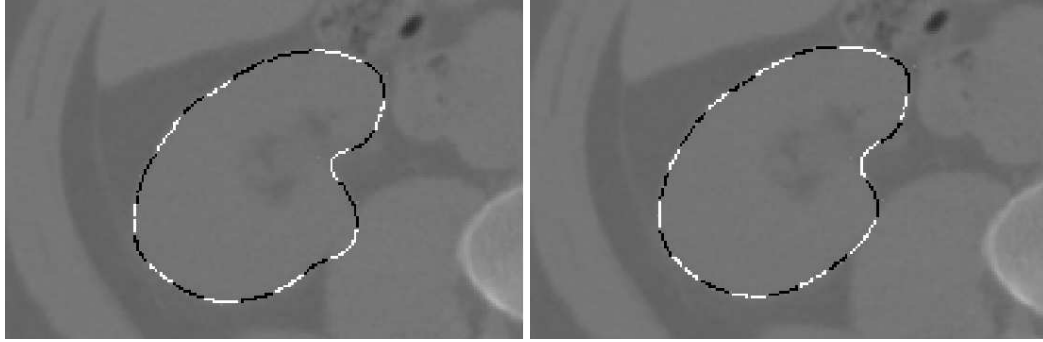


Figure 2: *left*: Results of converged B-Spline snakes without similarity force included. *right*: The same example of converged snakes with similarity forces included using parameter $\gamma = 0.3$.

We are using another improvement - classical curve representation is replaced by set of so called 'snaxels' with closed B-Spline curve. B-Spline curve as perfect tool for contour detection was introduced in [BHU00]. This approach reduces number of optimized parameters to coordinates of control points only. Using B-Spline implicitly brings benefit of intrinsic regularization property. B-Spline snakes with a very efficient computational scheme are presented in work of Jacob et al [JBU04].

3 ENERGY MODEL

We utilize a flexibility of snakes framework and we tried to find new terms which can be incorporated into it. We based our energy model based on regions. Contours in our model are represented by B-Spline curves.

In our first attempt we extend formula by an additional term which describes relation to the adjacent slices in CT dataset. This relation is based on a shape similarity measure. We are trying to find the best measure which is able to reduce unwanted behavior of the evolving curve.

$$E(s) = E_{region1}(s) + \gamma \cdot similarity(s, s_{neighbour}) \quad (2)$$

We tried to find how to express local high frequency changes of a shape in the similarity measure. This criterion can indicate overflow of the contour to a adjacent area through 'bridges' of similar intensity. These bridges should be narrow enough to be rendered as high frequency. High frequency can rise the similarity term in our formulation (2). Minimization scheme can isolate and eliminate them because of their significant differences. We construct shape describing vector as Fourier power spectrum of boundary orientation angle changes. Similarity of two shapes is equal to l_2 -distance of their shape vectors. It is used as *similarity* term in (2). In [LAL03] it was shown that this similarity measure is sensitive to significant differences of corresponding parts of curves.

Simple Chan and Vese region energy scheme (1) incorporates square distance from mean, which is very

rough approximation of inverted probability. Instead of this we are directly using probability of element classification to exterior or interior region in fashion of [JBU04]. Furthermore we simplify weight coefficients α and β to α and $(1 - \alpha)$ expressing balance between exterior and interior. It has only little importance in the new scheme.

$$E_{region2}(s) = -\alpha \int_{int(s)} \log(P_{int}(f)) - (1 - \alpha) \int_{ext(s)} \log(P_{ext}(f)) \quad (3)$$

Probability in (3) can be approximated by normal distribution from analysis of initial shape position. We can also completely rely on user's initial input and use normalized and optionally smoothed histogram of areas (interior, exterior) as our probability distributions. There are other interesting region-based energy models introduced in [JTW99].

$$E_{region3}(s) = -\frac{1}{2}(\rho_{int}^2 - \rho_{ext}^2)^2 \quad (4)$$

$$E_{region4}(s) = -\frac{1}{2}(\mu_{int}^2 - \mu_{ext}^2)^2 \quad (5)$$

Minimization itself can be achieved by the gradient descent method. Partial derivatives of functional E by parameters \mathbf{x} of the contour are the only terms to compute.

$$s_{n+1} = s_n + \delta \cdot \nabla_{\mathbf{x}} E(s(\mathbf{x})) \quad (6)$$

These parameters are in our case identical to control points of B-Spline curve. The most important feature of the region-based snake segmentation is possibility of reducing computational complexity from computing an area integral to computing a curve integral using Green's theorem.

We did not follow an example of [CV01] adding more than two types of energy functionals. It encounters

problem of energy equivalence which can not be always completely solved by parameters tuning. We can not simply (in meaning of linear relation) answer a question of how much region energy is equivalent to a unit of gradient based edge energy, length or area energy.

4 B-SPLINE CURVES

B-Spline curves are well known splines using polygonal base functions with limited support, which gives them great local control property. There are few problems we should handle with.

First is that we must use B-Splines in all energy functionals in place of a contour s . If we work with points on the contour and their displacement during the minimization step we must use control points only. It is a big advantage because there are fewer of them than contour points even if sampling is very rough.

First one - we must use B-Splines in all energy functionals in place of a contour s . If we are working with points on the contour and their displacement during the minimization step we must use control points only. This is a big advantage because there are fewer of them than contour points, even if sampling is very rough.

Order of B-Spline is another question. Cubic B-Spline is good enough for our purpose.

Number of control points or number of B-Spline sections depends on length of the whole closed contour. We define minimal and maximal length of segment and during iterations we check the length. If our limits are exceeded we split segment or merge adjacent segments as necessary.

The last problem relates to intersections. Sometimes evolving curve happens to be self-intersecting. For example if we are segmenting shape with holes, curve always intertwines around the hole and cycles forever. One solution consists in detecting intersections and breaking off parts of the curve. Free ends of the bigger part of the curve will be stucked together and the rest can be thrown away. We could also use the rest of the curve as an inner structure segmentation. This can be seen when segmenting higher or lower parts of kidney, which has pelvis in the middle (pelvis has very different tissue density). We might ignore it first time and later we can segment it by simple thresholding. Intersection detection can use convex wrapper property of B-Spline segments for computation speedup.

In [JBU04] they use integration of angle changes which gives various multiples of 2π depending on number and direction of loops. This method is detecting loops which implicate self-intersections, but is ineffective in cases described above.

5 SEGMENTATION PROCEDURE

We are trying to segment 3D volume using separate segmentation of each slice. Shape similarity measure is used as inter-slice relation which binds adjacent slices

together. Reasons for our preference to this scheme (compared to pure 3D deformable model technique like Active Surfaces) are inhomogeneous data and computational efficiency which is far better in the case of 2D techniques. We are working with datasets of voxels which are larger in one dimension than in other two. In case of pure 3D technique, evolution in two different directions could be incomparable. This approach offers almost interactive response and better user control (better than editing 3D surface control points).

Our segmentation procedure starts specifying top and bottom end points of segmented organ by a user. Optionally user can set other points in slices between top and bottom ends, which can help to determine starting positions. Starting positions on other slices are placed automatically between these which were set manually by the user. Initial shape is defined as small circle around these points. Probability distribution is estimated from area inside these circles. It is important to put them in the right place inside segmented organ. The user can optionally supply probability distribution from manually segmented shape in one slice.

Iteration starts after shape initialization and placement on each slice. In each iteration of the procedure we perform one step of snake energy minimization. Thanks to this scheme the whole object is changing its shape during segmentation process and thus can be observed and possibly corrected by the user. After one of slices converges it became steady point for its neighbors and is available for use in similarity term in equation (2). Neighbors of already converged slices are restricted by similarity in their further evolution. This scheme works well for rounded organs whose axial slices do not change topology and shape variation too rapidly.

6 RESULTS

Convergence of the basic model (2) is strongly dependent on parameters α, β, γ . The model (3), if supplied with proper probability distribution, gives very promising results. Our improvement with similarity measure can help to hold a curve in correct shape as can be seen in Figure 2.

We are working with native images of a kidney checkup and also with images of the same checkup with an contrast agent in several phases of satiation. In each case different strategy in parameter setting and probability distribution should be used to obtain optimal result. Native images work well with approximation by normal distribution. But in a case of thin patient lacking of contrast inter-organ fat, it is almost impossible to find a distribution which prevents overflowing to neighbouring organs without losing too much tissue on the surface of segmented organ. Using this scheme on slightly satiated kidney we are able to segment the whole organ and determine its volume well. Figure 4 shows final results

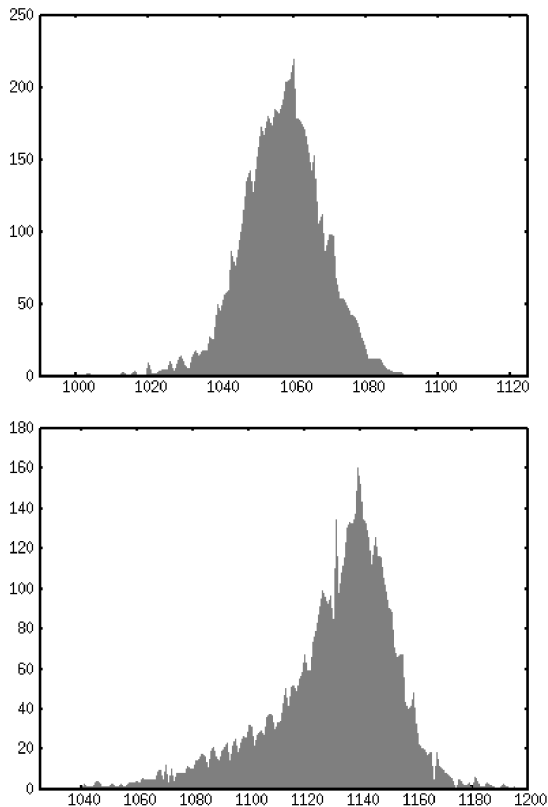


Figure 3: Histograms of segmented shapes. First graph from native CT corresponds to normal distribution. Second graph from an image with medium saturation of the contrast agent demonstrates slightly skewed distribution.

of our efforts. The approximation by normal distribution fails on a highly satiated kidney because it does not correspond to reality as shown in Figure 6. On the other side fine-tuned probability distribution works well on majority of patients.

A speed of the segmentation procedure is satisfying. Processing of a five-millimeter thick slices dataset takes about 80-90 seconds (intersection check is performed after each 40 iterations, convergence is achieved after about 400 iterations). On a two-millimeter slices dataset it takes 160 seconds, but the measurement is more precise. Time measurements were done on AthlonXP 2600+ computer.

7 CONCLUSION AND FUTURE WORK

We proved that our task can be effectively solved by segmentation using deformable models. Building efficient scheme for faster automatic segmentation will be our next goal. We have improved our framework by incorporating methods based on Green's theorem which speed up computations of region integral and its derivative. Detecting self-intersection is the slowest component of our algorithm, but also introduces simple topol-

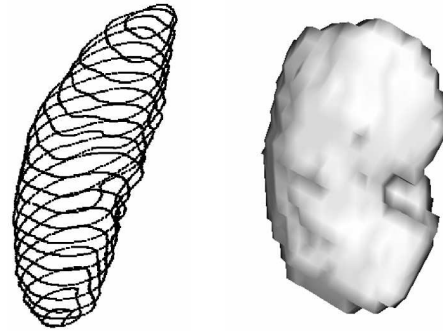


Figure 4: Schematic model(left) and 3D model(right) of segmented kidney.

ogy control (detection of holes). We are going to implement other enhancements like parallel computation of distant slices or multi-scale computations. Results of our measurements will be evaluated and assessed by medical specialist to determine its accuracy and possible usability in practice.

ACKNOWLEDGEMENTS

This work is supported by GAUK grant No. 359/2006 (Charles University in Prague). MUDr. Martin Horák from Bulovka Hospital in Prague is providing us with all necessary data, medical knowledge and experience.

REFERENCES

- [BHU00] Brigger, P., Hoeg, J., and Unser, M. (2000). B-Spline snakes: A flexible tool for parametric contour detection. *IEEE Transactions on Image Processing*, 9(9):1484–1496.
- [CV01] Chan, T. and Vese, L. (2001). Active contours without edges. *IEEE Trans. Image Processing*, 10(2):266–277.
- [JBU04] Jacob, M., Blu, T., and Unser, M. (2004). Efficient energies and algorithms for parametric snakes. *IEEE Transactions on Image Processing*, 13(9):1231–1244.
- [JTW99] Jr, A. Y., Tsai, A., and Willsky, A. (1999). A statistical approach to snakes for bimodal and trimodal imagery. In *ICCV '99: Proceedings of the International Conference on Computer Vision-Volume 2*, page 898, Washington, DC, USA. IEEE Computer Society.
- [KWT88] Kass, M., Witkin, A., and Terzopoulos, D. (1988). Snakes: Active contour models. *International Journal of Computer Vision*, 1(4):321–331.
- [LAL03] Lee, D., Antani, S., and Long, L. R. (2003). Similarity measurement using polygon curve representation and fourier descriptors for shape-based vertebral image retrieval.